International Journal of Engineering Trends and Technology
ISSN: 2231 – 5381 /doi:10.14445/22315381/IJETT-V70I1P221
Volume 70 Issue 1, 185-191, January, 2022

An Original Method of Extraction Bands Based On Spectral And Spatial Characteristic To Reduce The Hyperspectral Image

Agouzal Mehdi[1], Merzouqi Maria[2], Moha Arouch[3]

[1]*Laboratory of Engineering, Industrial and Management of Innovation (IMMII), Faculty of Science and Technology, University Hassan 1st, Settat, Morocco*
[2] *Electronic Systems, Sensors, and Nanobiotechnologies (E2SN), ENSET Mohammed V University Rabat, Morocco*
[3]*Laboratory of Engineering, Industrial and Management of Innovation (IMMII), Faculty of Science and Technology, University Hassan 1st, Settat, Morocco*

[1]agouzal.mehdi@gmail.com., [2]maria.merzouqi@um5s.net.ma, [3]Moha.arouch@uhp.ac.com.

Abstract *- Reducing the dimensionality of HIS* [1] *is still a hot topic and a challenge to be won. Numerous studies have been devoted to this objective, using different strategies to find an efficient and rapid method. The effectiveness of an approach in this area refers to the ability to optimize the number of bands without loss of information and to improve classification performance. Well-known methods treat spatial and spectral image characteristics separately. However, the combined treatment of these characteristics turned out to be another aspect to be highlighted* [2]. *In this article, a new reduction method is proposed, which is based on the fusion of the spatial-spectral characteristics. Specifically, it allowed the extraction of the spatial-spectral characteristic for all pixels. Then a measurement of the similarity of the spectral signatures is performed by the external spectral correlation to discern the unwanted bands. Then, discriminant analysis of the set selected from the first step is established by calculating the variance. After the descending ordering of the values of the variance of the spectral signatures of each pixel relative to the reference signature of each class, an adjustable selection percentage is used to count the repetition rate of the top brands in all classes to promote extraction performance while controlling the redundancy penalty. This method made it possible to reproduce a thematic map closer to the ground truth of Pavia. The experimental results obtained by SVM-RBF demonstrate the efficiency of the proposed method, whereby the total number of bands has been reduced from 103 to 35 with OA greater than 93%*

Keywords - *Reduction of dimensionality, Extraction method, Correlation, Variance, Spectral Signature, classification, RBF-SVM.*

I. INTRODUCTION

With the development of spectroscopes [3], the sensors became able to capture a new image known as a hyperspectral image. It has become an indispensable tool in human life. Thanks to its high resolution and its large number of spectral bands that have distinguished it. The hyperspectral image (IHS) can capture hundreds of bands that are strongly correlated with narrow spaced apart. This immense number of bands forms an image stack that discriminates between objects with subtle spectral divergence. It was able to overwhelm almost all areas, namely urban [4][6], soil [5], agriculture, medical [6], forest [7], etc.

However, its colossal number of brands represents a double-edged sword in front of its good exploitation, according to different measures (storage, compression, pre-treatment, treatment, classification...). This stack is made up of informative and redundant, and non-informative (noisy) bands, which make it process a difficult task. This acts directly on computational complexity and classification efficiency. Where a large number of labeled samples disrupts inductive algorithm learning and causes "dimensionality curse" [8] misclassification, so it seems reasonable to reduce its dimensionality in such ways as preserving information bands and discriminating complementary and unnecessary redundancy in order to get rid of it and eliminate noise [9]. In the same context, several reduction methods have been proposed in the literature, which can be categorized according to two strategies, either by selection or by extraction.

These are generally done using three basic approaches (filter [10], wrapper [11] [12] [13] Embedded [14]). For the same objective, that serves to reduce the dimensionality of HIS. A new filter approach is introduced, which performs the extraction[15] [16] of the relevant bands and the discrimination between the redundancies while eliminating the other unnecessary bands. This article will be structured as follows: the following section is devoted to giving the definitions relating to the proposed method, as well as the set of data used. The third section details the suggested methodology. Section 4 describes the study area and the used tools giving the used classifier and the user data. The results obtained and their analysis will be presented in section 5. Finally, the conclusion is drawn in Section 6.

II. INFORMATION RELATING TO THE CONTEXT

The Hyperspectral Image (HSI) is presented as a three-dimensional cube made up of 2D (XY) spatial information and other 1D (λ) spectral. The symbols (X, λ, Y) respectively specify the spatial height, the number of spectral bands, and the spatial width of the hypercube [17].

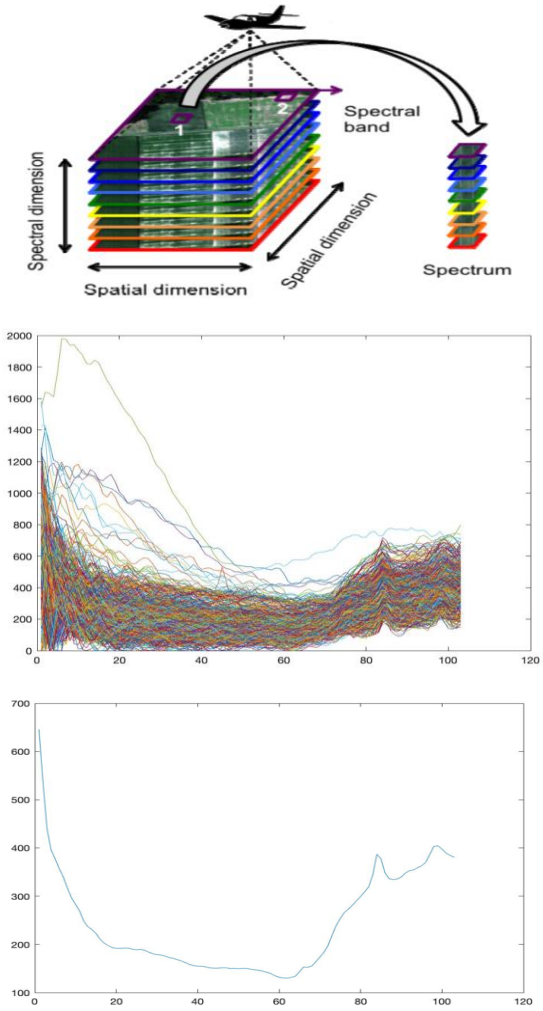

Fig 1. Hyperspectral image acquisition; the spectral signature of each pixel of class 9; the reference signature of class 9(shadows).

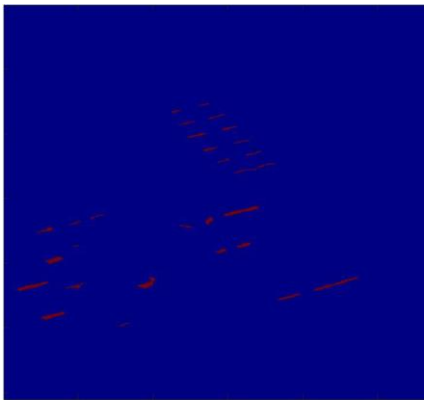

Fig 2 . Class 9 (Shadow) display in Pavia ground truth

The IHS consists of a number of N bands, can be represented as a matrix $\lfloor X_{xy}, N_{\lambda} \rfloor$.

Each pixel vector is denoted X_{xy} (x = i 1, 2…, n), and (y = i 1, 2… m), where n denotes the number of pixels in the spatial dimension of the image. Each pixel X_{xy} belongs to a class (k = 1, 2…, C), with C being the number of classes and N_{λ} the number of bands used [18] [19]. The initial form of this image is said to be relatively unintelligible. In addition, the reduction of the dimensionality of IHS is an essential step; it roughly allows:

- Ensure a good visualization and representation in order to understand and explore data provided by this hyperspectral image.
- Facilitate the analysis in order to identify and extract the relevant information.
- Guarantee the correct classification.
- Map the image in a plane lower than the original.

This reduction can be done according to two methods already named: the extraction [20] of attributes that require the transformation or the projection of the original data to a new reduced subspace. Usually, this transformation tarnishes the original shape of the data, resulting in the loss of the original information. On the other hand, there is the attribute selection method [21], which makes it possible to distinguish the relevant attributes without making any transformations.

Alongside these methods, there is also another way to solve the problem of the hyperspectral image. According to the literature, many approaches have been adopted for the same goal, taking into account the two pieces of information provided by this image (spatial and spectral) [22]. As already known, each object or material has its spectral response (fingerprint) [23] that distinguishes it. This signature contains multiple pixels that are spatially strongly correlated and spectrally closely contiguous. However, exploring these two pieces of information in a reduction method is effective. Instead, there are approaches that merge information (spectral, spatial) that fall into three categories: feature-level fusion [24], decision-level fusion [25] [26], and regularization-based fusion [27].

For the first category (feature-level fusion), this method first makes it possible to independently extract the spectral and spatial features. At the level of a single vector, the extracted features are concatenated, then the construction of multiple Kernel functions according to its suitable characteristics. This technique was used for the determination of morphology profiles by [28]. On the other hand, the concatenation of these data requires a large space that can contain noisy or redundant data, which will lead to an over-adjustment and to the deterioration of the performance of the classification. As a general summary, it should be stated that this fusion is relatively difficult to achieve in practice since it cannot be controlled by precise methods of extraction and concatenation. This diversity leads to feature incompatibility, and even the

correspondence between different feature spaces may be unknown. Second category (decision-level fusion) results are obtained from spatial and spectral information, respectively [29]. This method is effective if the image has a large spatial structure. However, this technique requires good image segmentation [30], as the results rely heavily on the high accuracy of the primitive segmentation results, which is a difficult task for hyperspectral images. The last category (merging based on regularization) usually relies on a regularizer that represents the spatial information in the original objective function.

The hyperspectral image consists of several classes. Each class is defined by labeled pixels taken from hundreds of spectral bands ranging from the visible to the infrared electromagnetic spectrum. In general, the spectral signature of each pixel can be directly used as a classification characteristic [31]. However, the unique exploitation of these spectral characteristics provided by the immense quantity of the pixels fiercely correlated at the spectral level is often insufficient for a good classification. Thus, spatial contextual information is also useful for classification [32] [33].

In this regard, we will focus in this article on the decision-level fusion method. This work proposes a new method of extracting unnecessary bands while being based on the fusion of spectral-spatial characteristics. Eventually, most of the supported methods are based on the vector representation of the features in an independent way, which results in an undeniable loss of the inherent connection between them. To overcome this type of issue, the introduced method is based on reverse engineering applying an extraction of spectral and spatial information from the ground truth while calculating two scores: inter-correlation by the Pearson correlation coefficient [34] and the variance according to the SBS principle (Sequential Backward selection) which is used to eliminate unwanted bands from the candidate set in order to extract only the relevant bands [35].

A. Pearson coefficient (correlation):

The correlation coefficient makes it possible to have a synthetic measure of the intensity of the linear dependence relation between two variables while determining their direction if this relation is monotonic. In the case of hyperspectral images, it is calculated according to two types: inter-bands, which designates the measure of the correlation at the spatial level (the variables are bands). Also, find intra bands that are calculated at the spectral level where the variables will be classes, pixels in a band. In this work, the correlation adopted is spectral. It determines the unwanted bands from the spectral response of each pixel of each class for all bands. The formula below presents the Pearson coefficient, which has as the numerator the covariance of two variables and as the denominator the product of their standard deviations (respectively) [36] [37].

$$Corr(A,B) = \frac{\operatorname{cov}(A,B)}{\sigma_A \sigma_B} = \frac{E\left[(A-\mu_A)(B-\mu_B)\right]}{\sigma_A \sigma_B}.$$

The value of this coefficient is often bounded by two values [-1 and 1]. A represents the signature carried by a candidate pixel, and B is the reference signature of the candidate class. To tighten the precision of the selection of the bands, a threshold has been set to be exceeded.

B. The variance measure:

It makes it possible to measure the dispersion of a probability distribution, some samples, values. It is expressed in several forms, namely the mean of the squares of the deviations from the mean, the difference between the mean of the squares of the values of the variable, and the square of the mean. The variance is always positive and only vanishes if the values are all equal. Its square root defines the standard deviation σ, hence the notation [38] [39].

$$Var = \frac{1}{n}\sum_{i=1}^{n}\left(x_i - \bar{x}\right)^2.$$

Where n is the number of the element and $\bar{x}$ the mean of an element x_i.

C. The homogeneity of GLCM

From the gray level co-occurrence matrix, we can extract several parameters like energy, contrast, correlation, homogeneity, and others. These parameters help to do the textural analysis. In this case, we introduce that the homogeneity, which is a statistical measure also for the comparison, is logical and which has other aspects. This parameter makes it possible to quantify the proximity of the distribution to the diagonal elements of the GLCM matrix [40]. Pixels are considered similar if they have large homogeneity values. It is calculated as follows:

$$Homogeneity = \sum_i \sum_i \frac{P_{ij}}{1+(i-j)^2}.$$

With P_{ij} is the Element i and j of the symmetric GLCM matrix [41].

III. PROPOSED METHODOLOGY

As well as detail said image consists of the hundreds of bands that cover different objects of the target scene presented by a set of classes. The number of classes is often negligible compared to the number of pixels. This inequality makes the selection of bands difficult. In particular, the acquisition of IHS takes place in closely spaced and strongly correlated bands, which explains the existence of redundant bands and others affected by noise. However, the proposed method is a supervised method that adopts the concept of reverse engineering. It eliminates irrelevant bands and reduces redundant bands, and extracts relevant bands. This approach typically builds on the principle of SBS selection for an extraction strategy that relies on merging spatial and spectral features while measuring two scores (correlation, variance) for reduction. All the bands retained will be evaluated by classifying the SVM-RBF [42] [43] as a primary classifier and the KNN [44] [45] as a secondary classifier in order to confirm the trend of the results obtained [15]. To also check the

credibility of this approach, we replaced the correlation with another measure that affects the texture of the image of the homogeneity extracted from the GLCM matrix, namely that the proposed method is extrinsic hence this method. Otherwise, we are acting on the appearance of the spectral characteristics and not on their contents. The algorithm process introduced will be presented below.

A. The rationale for the choice of correlation

The choice of this correlation coefficient is made by a distinction. According to work [], we had as a synthesis that the band correlated either directly or inversely with the ground truth means that it is informative said to be relevant. In order to properly control the redundancy, a correlation threshold = 0.9 has been fixed, chosen empirically. The figure below plots the correlation and mutual information of each band with the ground truth. From Figure 2, it can be seen that band 25 is closer to the ground truth and which has an important value in both measures correlation and mutual information. In addition, we also identify the last band, 97, which is not practically similar to the ground truth since the correlation is equal to 0 even though it has a large amount of information, so for an image to be relevant, it must maximize both measures. Even this is not the focal point in this study. This study focuses on the form and not the content of the image.

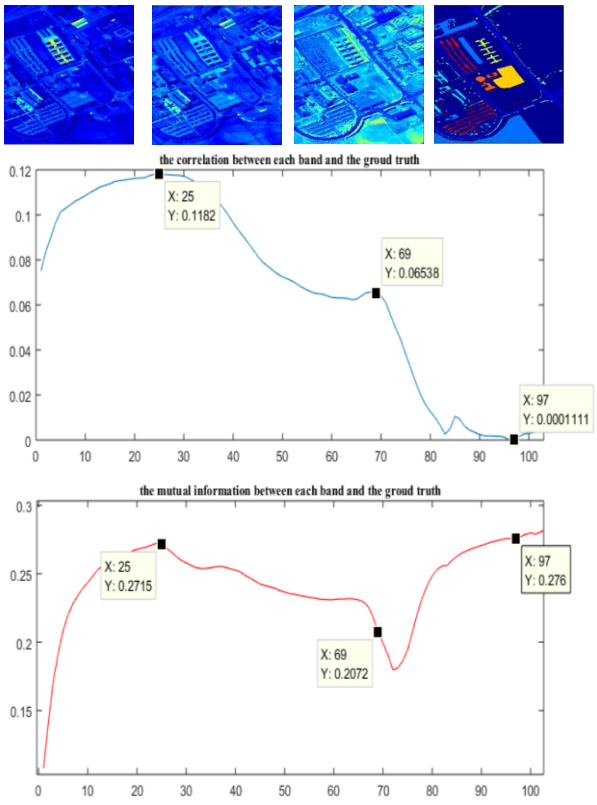

Fig 3. The image of mentioned bands. The curve of correlation of bands with the ground truth (Gt) and the mutuelle information with (GT).

B. The algorithm process

The algorithm process of the proposed method can be formulated as follows:

- The declaration of the input variables:
  - All the initial data: F.
  - The bands: B.
  - The ground truth: C.
  - Percentage of the selection.
  - S: all the bands to select;
  - SS: All the bands to be eliminated;
- Algorithm initialization: first stage.
  - $Th \leftarrow$ The correlation threshold for the redundancy check: 0.9;
  - $SS \leftarrow \{\}$ set of bands to be eliminated;
  - $S \leftarrow \{\}$ set of bands to be selected;
  - Segmentation of the bands in class according to the ground truth;
  - Extraction of the pixels (P_{ij}) of each class C_i ;
  - Extraction of the reference signature (S_r) of each class;
- Second stage: selection of the relevant bands
  - The computing of the correlation coefficient ($Corr$) of each pixel P_{ij} with the reference signature S_r of the concerned class C_i .
- ✓ A gourmet selection of relevance:
  - Repeat this step for all classes.
  - Checking the condition $Corr(P_i, S_r) \geq 0.9$.
  - Extract the relevant bands B_p that validate the condition.
  - Elimination of irrelevant bands B_r , which does not validate the condition.
  - Reset $F \leftarrow F \setminus \{B_p\}$, define $S \leftarrow \{B_p\}$, define $SS \leftarrow \{B_r\}$.
- ✓ Elimination of non-informative bands:
  - Calculates the variance between the signature of each pixel that does not validate the condition with the signature reference ().
  - Rank the variances in descending order.
  - Extraction of unwanted tops 5 bands from the signature, which have a high variance with the ().
  - Count the number of repetitions of these unwanted bands in all classes.
  - Verification of a selection condition: are the unwanted bands that repeat in all classes and that exceed an adjustable selection percentage P_{sa} .
  - Bands that exceed P_{sa} will be eliminated.
  - Reset $F \leftarrow F \setminus \{B_r\}$ define $S \leftarrow \{S, F\}$.
  - $S \leftarrow \{S, F\}$;
  - End of process.
- The classification process starts for the retained bands S with the SVM-RBF classifier.

IV. STUDY AREA AND USED TOOLS

A. *The used classifier (SVM-RBF/ KNN).*

According to a comparative study on the efficiency of classifieds in the classification of hyperspectral images, the SVM-RBF was always in the lead. Whatever the nature of the image, it was able to reach important values with minimum training samples. To evaluate and validate the results of this original approach, we adopted the SVM-RBF as the main classifier and the KNN as the secondary classifier.

The principle of operation of the SVM learning machine is based on the construction of optimal hyperplanes between classes by specifying the adequate margin of separation between the classes. Besides the kernels, the latter is also characterized by other parameters such as gamma, C, the training data, and the test data, which have been fixed at "scale, 512, 50% of the labeled classes are reserved randomly, 50 %" respectively.

In addition, another classifier has been added to definitively judge the results obtained. The KNN, which is a fast induction algorithm, is easy to master and cannot be configured. It is often used for supervised classification. It is determined by the number of neighbors, a fixed K, in this case, K = 5. Its operating principle is based on the determination of the distances between the reference entities illustrated by vectors and the classified entities.

These learning machines quantify the performance of precision by several metrics: Kappa coefficient (KA), overall precision (OA), average precision (AA), and others that have not been calculated [46].

• The Kappa coefficient (KA) qualifies the thematic map obtained after classification with the ground truth.

•

The overall precision remains a probability expressed as a percentage. It defines the correctness of the class mapping proportion. It is calculated by the sum of the predictions of the inductive algorithm (true positives and false positives), divided over all the samples tested).

• Average Precision (AA) shows the average value of the exact classification for all classes.

Table 1. The classification rate uses two classifiers for the proposed method, "Correlation Ratio."

Nbr of Sb	25	35	50	59	71	78	89
% of Sb	35%	30 %	25 %	20 %	15 %	10 %	5%
SVM-RBF							
OA (%)	93.55	93.91	94.15	94.26	94.70	95.02	95.33
AA (%)	91.43	91.49	91.90	92.12	92.76	92.95	93.25
Ka (%)	91.42	91.38	92.23	92.37	92.95	93.39	93.79
KNN- K=5							
OA (%)	91.42	91.78	92.23	92.37	92.95	93.39	93.79
AA (%)	89.65	90.08	89.89	90.20	90.84	91.06	91.65
Ka (%)	87.04	87.86	87.57	87.92	88.67	88.86	89.39

B. *Tools and dataset*

The algorithm used is programmed by the more popular MATLAB 2020a scientific programming language. This scripting language is often used for manipulating matrices, plotting curves, implementing algorithms on various fields, namely image processing. This algorithm was run on a MacBook Pro computer with a quad-core processor and Intel Iris Plus Graphics 655 1536 MB graphics processor, its macOS operating system with 8 GB of RAM.

This experiment was done on the ROSIS Pavia image. Pavia is acquired by the ROSIS-03 (Reflective Optics Imaging Spectrometer) sensor in active mode applying the "Pushbroom" technique. Pavia covers an urban side of the engineering school of the University of Pavia in Italy. It usually consists of 115 bands taken from the spectral range [0.43 to 0.86 µm]. After preprocessing and removing 12 bands affected by atmospheric noise, the final IHS Pavia contains only 103 bands of 610 × 340. The sum of the tagged pixels represents 20% of the total pixel count. 42776 pixels are labeled from 1 to 9 classes of provided ground truth [47].

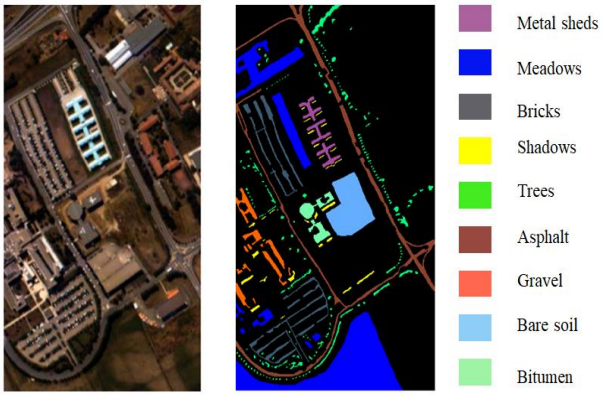

Fig 4 The Color composite of the labeled classes for the ground truth of Pavia and the real image of Pavia

V. RESULTS AND THEIR ANALYSIS

This section is devoted to the presentation of the obtained results with two classifiers for the only used hyperspectral image Pavia. Furthermore, it is also dedicated to discussing the results with the aim of extracting the final synthesis.

A. *Results*

Table 1 shows the results of extraction of the different subsets according to the proposed method, which is based on the correlation. According to the results obtained according to a different percentage of selection, one notes the effectiveness of the reduction of this algorithm by large values of the OA metric.

Nbr of Sb: Number of selected bands

% of Sb: Percentage of selection

Table 2 also shows the results of extraction of the different subsets of bands according to the proposed method of comparison, which is based on one of the parameters extracted from the GLCM matrix that is the Homogeneity. According to the results obtained according to a different percentage of selection, we find that this method is fewer notes the efficient than the proposed.

Table 2. The classification rate using two classifiers for the proposed method "Homogeneity."

Nbr of Sb	25	35	50	59	71	78	89
% of Sb	35%	30%	25%	20%	15%	10%	5%
SVM-RBF							
OA (%)	91.27	91.44	91.49	92.02	92.26	92.52	92.77
AA (%)	89.71	89.88	89.98	90.17	90.90	91.09	91.03
Ka (%)	88.75	88.91	89.43	89.78	89.93	90.41	90.31
KNN- K=5							
OA (%)	88.63	88.70	88.81	89.34	89.62	89.73	89.45
AA (%)	86.11	86.23	86.76	86.98	87.01	87.14	87.41
Ka(%)	84.02	84.33	84.32	85.19	85.32	85.79	85.72

B. Analysis of results

As an analysis of the results shown in Tables (1 and 2), we can see that the OA values obtained by the SVM are always higher compared to those obtained by the KNN. This affirms the relevance of the choice of the SVM for the classification in this case, and even for the reduction of the IHS in case of application of another method that requires the participation of the classifiers in the operations of the selection or extraction.

It can also be noted that the results obtained by the proposed method, which are based on the correlation with substantial performance. She was able to keep her progress, even during the algorithm relief. In other words, when the selection percentage was reduced, the number of bands increased, but this did not affect the performance of the precision; on the contrary, it contributed to the progression of the OA, which was able to achieve more than 95%. This comes down to the presence of the relevant redundancy that we call the complementary redundant, which has a positive role on the classifier.

To increase the ranking rate, we have allowed some redundancy using negative thresholds.

On the other hand, the method of comparison introduced, which is based on has the same structure and which measures the homogeneity, was able to overcome the dimension curse, yet their performances are lower than those obtained by the proposed method. This measure is said to have a weakness in redundancy discrimination.

Finally, as a general synthesis, these simulations show that the two measurements are effective for this method, which makes it possible to extract the relevant bands and eliminate the unwanted bands, except that the correlation has a remarkable privilege in front of the homogeneity, which consists in discerning and controlling the subsidiary redundancy. Taking the case where the tolerance of the redundant and remarkable 78 bands, the proposed method exceeded 95% for the OA and AA> 92% and ka> 93 with the SVM classifier. In addition, the results obtained by the KNN classifier, the proposed method reach more than 93% for the OA and AA> 91 and ka> 88. Nevertheless, the comparison method for the same number of bands could not reach 93 for the OA; hence the other metrics equal to AA = 91.09; ka = 90.42 with SVM. The KNN was not better either from SVM. The values of the metrics are 89.73; 87.14; 85.79.

VI. CONCLUSION

This work proposes an original extraction approach based on reverse engineering. It has demonstrated its effectiveness with excellent performance. This method applies the SBS technique for Pavia hyperspectral image reduction. According to the observed experimental results and the curves which trace the pace of the progression of the overall precision of the above classification, it is claimed that this approach was able to overcome the famous IHS constraint, the Hughes phenomenon. We were able to reduce the overall number by more than 50%, with a high OA exceeding (+ 94%). On the other hand, the comparison method experienced deterioration in results compared to the main one. Even the algorithmic principle is the same, except that we replaced correlation with homogeneity to measure contextual information.

To conclude, measuring internal or external correlation consistently shows superior individual performance in distinguishing between bands. Thus, the association of the correlation between the appearance of the signatures and their variance makes it possible to extract the unwanted bands (redundant, noisy) and to preserve the desirable ones while tolerating the additional redundancy by adjusting the final selection percentage. The obtained results give the motivation to develop this method as a perspective for this work. Thinking to include other measures such as distances, other characteristics like energy sensibility homogeneity. Also, touching other aspects such as texture or training the mixed pixels and applying a different approach such as l integration of the classifier in the reduction process either by (cover or hybrid).

ACKNOWLEDGMENT

Many thanks to M Graña, MA Veganzons, B Ayerdi for hyperspectral Dataset from Grupo De inteligencia Computacial (GIC).

REFERENCES

[1] T. Tr, Dimensionality Reduction: A Comparative Review, 36.

[2] Q. Man, P. Dong, and H. Guo, Pixel- and feature-level fusion of hyperspectral and lidar data for urban land-use classification, Int. J. Remote Sens., 36(6) (2015) 1618–1644.

[3] C.-I. Chang, Ed., Hyperspectral data exploitation: theory and applications. Hoboken, N.J: Wiley-Interscience, (2007).

[4] E. Adam, O. Mutanga, and D. Rugege, Multispectral and hyperspectral remote sensing for identification and mapping of wetland vegetation: a review, Wetl. Ecol. Manag., 18(3) (2010) 281–296.

[5] F. D. van der Meer et al., Multi- and hyperspectral geologic remote sensing: A review, Int. J. Appl. Earth Obs. Geoinformation, 14(1) (2012) 112–128.
[6] B. Fei, Hyperspectral imaging in medical applications, in Data Handling in Science and Technology, 32 (2020) 523–565.
[7] O. Mutanga, E. Adam, and M. A. Cho, High-density biomass estimation for wetland vegetation using WorldView-2 imagery and random forest regression algorithm, Int. J. Appl. Earth Obs. Geoinformation, 18 (2012) 399–406.
[8] G. Hughes, On the mean accuracy of statistical pattern recognizers, IEEE Trans. Inf. Theory, 14(1) (1968) 55–63.
[9] M. Hasanlou and F. Samadzadegan, Comparative Study of Intrinsic Dimensionality Estimation and Dimension Reduction Techniques on Hyperspectral Images Using K-NN Classifier, IEEE Geosci. Remote Sens. Lett., 9(6) (2012) 1046–1050.
[10] J. Huang, Y. Cai, and X. Xu, A Filter Approach to Feature Selection Based on Mutual Information, in 2006 5th IEEE International Conference on Cognitive Informatics, Beijing, China, (2006) 84–89.
[11] Jinjie Huang, Yunze Cai, and Xiaoming Xu, A Wrapper for Feature Selection Based on Mutual Information, in 18th International Conference on Pattern Recognition (ICPR'06), Hong Kong, China, (2006) 618–621.
[12] M. Merzouqi, E. Sarhrouni, and A. Hammouch, Classification and Reduction of Hyperspectral Images Based on Motley Method, in Intelligent Systems Applications in Software Engineering, vol. 1046, R. Silhavy, P. Silhavy, and Z. Prokopova, Eds. Cham: pringer International Publishing, (2019) 155–164.
[13] M. Merzouqi, H. Nhaila, E. Sarhrouni, and A. Hammouch, Improved filter algorithm using inequality fano to select bands for HSI classification, in 2015 Intelligent Systems and Computer Vision (ISCV), Fez, Morocco, (2015) 1–5.
[14] R. Archibald and G. Fann, Feature Selection and Classification of Hyperspectral Images With Support Vector Machines, IEEE Geosci. Remote Sens. Lett., 4(4) (2007) 674–677.
[15] M. Agouzal and M. Arouch, A new method for hyperspectral reduction based on the trend of the electromagnetic range, in 2020 Fourth World Conference on Smart Trends in Systems, Security and Sustainability (WorldS4), London, United Kingdom, (2020) 782–787.
[16] X. Kang, S. Li, and J. A. Benediktsson, Feature Extraction of Hyperspectral Images With Image Fusion and Recursive Filtering, IEEE Trans. Geosci. Remote Sens., 52(6) 3742–3752 (2014).
[17] X. Ceamanos and S. Valero, Processing Hyperspectral Images, in Optical Remote Sensing of Land Surface, Elsevier, (2016) 163–200.
[18] P. Mishra, M. S. M. Asaari, A. Herrero-Langreo, S. Lohumi, B. Diezma, and P. Scheunders, Close range hyperspectral imaging of plants: A review, Biosyst. Eng., 164 (2017) 49–67.
[19] J. M. Bioucas-Dias, A. Plaza, G. Camps-Valls, P. Scheunders, N. Nasrabadi, and J. Chanussot, Hyperspectral Remote Sensing Data Analysis and Future Challenges, IEEE Geosci. Remote Sens. Mag., 1(2) (2013) 6–36.
[20] C. Lee and D. A. Landgrebe, Feature extraction based on decision boundaries, IEEE Trans. Pattern Anal. Mach. Intell.,15(4) (1993) 388–400.
[21] T. H. Dat and C. Guan, Feature Selection Based on Fisher Ratio and Mutual Information Analyses for Robust Brain-Computer Interface, in 2007 IEEE International Conference on Acoustics, Speech and Signal Processing - ICASSP '07, Honolulu, HI, USA, (2007) I-337-I–340.
[22] M. Fauvel, Y. Tarabalka, J. A. Benediktsson, J. Chanussot, and J.C.Tilton, Advances in Spectral-Spatial Classification of Hyperspectral Images, Proc. IEEE, 101(3) (2013) 652-675.
[23] C. F. Lam and D. Kamins, Signature recognition through spectral analysis, Pattern Recognit., 22(1) 39–44 (1989).
[24] C. Xu, I. Kim, and S. G. Kong, Feature level fusion for hyperspectral images, Orlando, Florida, USA, May (2009) 73150N.
[25] B. Bigdeli, F. Samadzadegan, and P. Reinartz, A decision fusion method based on multiple support vector machine system for fusion of hyperspectral and LIDAR data, Int. J. Image Data Fusion, 5(3) (2014) 196–209.
[26] O. Sharifi, M. Mokhtarzadeh, and B. Asghari Beirami, A new deep learning approach for classification of hyperspectral images: feature and decision level fusion of spectral and spatial features in multiscale CNN, Geocarto Int., (2021) 1–26.
[27] M. M. Khattab, A. M. Zeki, A. A. Alwan, and A. S. Badawy, Regularization-based multi-frame super-resolution: A systematic review, J. King Saud Univ. - Comput. Inf. Sci., 32(7) (2020) 755–762.
[28] V. De Witte, G. Thoonen, P. Scheunders, A. Pizurica, and W. Philips, Classification of multi-source images using color morphological profiles, in 2011 IEEE International Geoscience and Remote Sensing Symposium, Vancouver, BC, Canada, (2011) 3919–3922.
[29] Y. Nanyam, R. Choudhary, L. Gupta, and J. Paliwal, A decision-fusion strategy for fruit quality inspection using hyperspectral imaging, Biosyst. Eng., 111(1) (2012) 118–125.
[30] A. Tamim, Segmentation et classification des images satellitaires: application à la détection des zones d'upwelling côtier marocain et mise en place d'un logiciel de suivi spatiotemporel, 93.
[31] K. Wang, X. Gu, T. Yu, Q. Meng, L. Zhao, and L. Feng, Classification of hyperspectral remote sensing images using frequency spectrum similarity, Sci. China Technol. Sci.,56(4) (2013) 980–988.
[32] J. Yue, W. Zhao, S. Mao, and H. Liu, Spectral–spatial classification of hyperspectral images using deep convolutional neural networks, Remote Sens. Lett., 6(6) (2015) 468–477.
[33] Y. Tarabalka, J. A. Benediktsson, J. Chanussot, and J. C. Tilton, Multiple Spectral–Spatial Classification Approach for Hyperspectral Data, IEEE Trans. Geosci. Remote Sens., (2010) 5570985.
[34] H. Akoglu, User's guide to correlation coefficients, Turk. J. Emerg. Med., 18(3) (2018) 91–93.
[35] S. J. Reeves and Zhao Zhe, Sequential algorithms for observation selection, IEEE Trans. Signal Process., 47(1) (1999) 123–132.
[36] J. Zhao et al., FeatureExplorer: Interactive Feature Selection and Exploration of Regression Models for Hyperspectral Images, in 2019 IEEE Visualization Conference (VIS), Vancouver, BC, Canada, (2019) 161–165.
[37] P. Lasch and I. Noda, Two-Dimensional Correlation Spectroscopy for Multimodal Analysis of FT-IR, Raman, and MALDI-TOF MS Hyperspectral Images with Hamster Brain Tissue, Anal. Chem., 89(9) (2017) 5008–5016.
[38] S. Bourennane, C. Fossati, and A. Cailly, Improvement of Classification for Hyperspectral Images Based on Tensor Modeling, IEEE Geosci. Remote Sens. Lett.,7(4) (2010) 801–805.
[39] M. R. Gupta and N. P. Jacobson, Wavelet Principal Component Analysis and its Application to Hyperspectral Images, in 2006 International Conference on Image Processing, Atlanta, GA,(2006) 1585–1588.
[40] F. Mirzapour and H. Ghassemian, Improving hyperspectral image classification by combining spectral, texture, and shape features, Int. J. Remote Sens., 36(4) (2015) 1070–1096.
[41] S. Singh, D. Srivastava, and S. Agarwal, GLCM and its application in pattern recognition, in 2017 5th International Symposium on Computational and Business Intelligence (ISCBI), Dubai, United Arab Emirates, (2017) 20–25.
[42] R. Eyraud, Classification, Apprentissage, Décision, 30.
[43] B.-C. Kuo, H.-H. Ho, C.-H. Li, C.-C. Hung, and J.-S. Taur, A Kernel-Based Feature Selection Method for SVM With RBF Kernel for Hyperspectral Image Classification, IEEE J. Sel. Top. Appl. Earth Obs. Remote Sens.,7(1) (2014) 317–326.
[44] S. Zhang, X. Li, M. Zong, X. Zhu, and D. Cheng, Learning k for kNN Classification, ACM Trans. Intell. Syst. Technol., 8(3) (2017) 1–19.
[45] M. Maria, S. El Kebir, and H. Ahmed, Reduction dimensionality of hyperspectral imagery using genetic algorithm and mutual information and normalized mutual information as a fitness function, Int. Rev. Appl. Sci. Eng., 12(1) (2021) 64–75.
[46] M. Maria, Reduction of the Hyperspectral images Dimensionality Using a New Genetic Algorithm Procedure, 15(3) (2020) 12.
[47] R. Doerffer, B. Kunkel, and H. van der Piepen, Rosis - An Imaging Spectrometer For Rejiote Sensing Of Chlorophyll Fluorescence, Los Angeles, CA, United States, (1989) 36.
[48] M, Merzouqi, M, Agouzal, E, Sarhrouni, A, Hammouch. A study of a proposed suboptimal selection strategy based on genetic algorithm and filters of mutual information. International Journal of Engineering Trends and Technology (IJETT), 69(11) (2021).